JMBFS

Journal of Microbiology, Biotechnology and Food Sciences

International peer-reviewed scientific online journal

Published by Faculty of Biotechnology and Food Sciences

INHIBITORY EFFECTS OF *STERCULIA LYCHNOPHORA* HANCE ETHANOL EXTRACTS ON BIOFILM FORMATION AND VIRULENCE FACTORS OF *PSEUDOMONAS AERUGINOSA*

Ta Ngoc Ly[1], Hsin-Yi Hung*[2], Nguyen Tu Quyen*[1]

Address(es):
[1] The University of Da Nang - University of Science and Technology, Danang 550000, Vietnam.
[2] School of Pharmacy, College of Medicine, National Cheng Kung University, Tainan 70101, Taiwan.

*Corresponding author: tnly@dut.udn.vn

https://doi.org/10.55251/jmbfs.10483

ARTICLE INFO

Received 17. 8. 2023
Revised 1. 3. 2024
Accepted 11. 3. 2024
Published 1. 6. 2024

Regular article

OPEN ACCESS

ABSTRACT

This study aimed to explore the inhibitory effects of dried fruit ethanol extracts of *Sterculia lychnophora* Hance (SLHe), a traditional medicinal plant known as Pangdahai, on biofilm formation and virulence factors of *Pseudomonas aeruginosa*. Screening of bioactive compounds extracted from *Sterculia lychnophora* revealed a strong binding affinity to anthranilate-CoA ligase (PqsA), which regulates genes involved in pyocyanin production and biofilm formation. The experimental investigation confirmed the inhibitory effects of SLHe on biofilm formation and its ability to disrupt existing biofilms. Additionally, SLHe exhibited reductions in pyocyanin production and protease activity of *Pseudomonas aeruginosa*. These findings indicate the therapeutic potential of SLHe as a natural alternative for treating bacterial infections, particularly those associated with bacterial biofilm formations.

Keywords: anthranilate-CoA ligase, biofilm formation, pyocyanin, *Pseudomonas aeruginosa*, *Sterculia lychnophora*

INTRODUCTION

Sterculia lychnophora Hance belongs to the Sterculiaceae family. The trees grow mainly in tropical zones, including Vietnam, India, Malaysia, Thailand, Indonesia, and Taiwan **(Oppong, LI, *et al.*, 2018)**. *S. lychnophora* fruit is elliptic, about 2.0-2.5 cm long, and 1.1-1.5 cm in diameter. The seed's outer layer is very thin and brittle, and when soaked in water, its exposed interior is yellowish brown with a spongy mucus-rich consistency. The decoctions of dried fruit have been traditionally used for the treatment of sore throat, toothache, constipation, cough, menorrhagia, and pain **(Li, 2015; Oppong, LI, *et al.*, 2018)**. In particular, *S. lychnophora* is famous for preventing and treating pharyngitis. Scientific exploration has illuminated the multifaceted pharmacological repertoire of *S. lychnophora*. In-depth investigations spanning in vitro and in vivo realms have underscored its antimicrobial potential, offering promise for therapeutic interventions against various pathogens (**Palve *et al.*, 2016**). Additionally, *S. lychnophora* has exhibited ulcer-protective attributes ***(Ogale et al.*, 2014)**, tumor suppressive **(Kawk *et al.*, 2021),** and weight loss facilitation **(Panomai, 2018).** The neuroprotective capacity of *S. lychnophora* has also been documented, underscoring its relevance in neurological health maintenance **(R. F. Wang *et al.*, 2013)**. The bioactive richness of *S. lychnophora* is evident in its constituent repertoire. Noteworthy compounds isolated from this botanical marvel include alkaloids **(R.-F. Wang *et al.*, 2003)**, flavonoids **(Zhao *et al.*, 2008)**, polysaccharides **(Wu *et al.*, 2012)**, cerebrosides ***(R. F. Wang et al.*, 2013)** and steroids **(Pimpliskar, 2014)**. These compounds collectively contribute to the plant's diverse pharmacological effects.

Bolstered by its pharmacological profile, *S. lychnophora* finds an intriguing place in the culinary and gastronomic realms. When steeped in boiling water, the seeds yield a distinctive tea cherished for its flavors and potential health benefits. Alternatively, the extracted flesh, combined with sugar, ice, and basil seeds soaked in water, culminates in a rejuvenating beverage. This concoction offers a refreshing delight, infused with pandan, cinnamon, ginger, and licorice and delicately sweetened with brown sugar. Beyond beverages, *S. lychnophora* integrates seamlessly into culinary arts, enhancing delicacies like puddings and cakes with its unique essence **(Oppong, LI, *et al.*, 2018)**.

Pseudomonas aeruginosa emerges as a prominent causative agent of nosocomial infections, significantly burdening global healthcare systems. Manifesting a diverse array of infections, including respiratory tract, urinary tract, wound, and bloodstream infections, *P. aeruginosa* has garnered substantial attention **(Qin *et al.*, 2022)**. This bacterium exhibits numerous virulence factors, including the production of exotoxins, biofilm formation ability, and antibiotic resistance **(Liao *et al.*, 2022)**. Notably, the distinctive structure of quorum sensing (QS) and biofilm formation fuels the antimicrobial resistance observed in *P. aeruginosa* **(Díaz-Pérez *et al.*, 2023)**. These biofilms, intricate microbial communities enshrouded in an exopolysaccharide matrix, confer robust resistance against host immune responses and therapeutic interventions **(Vestby *et al.*, 2020).** *P. aeruginosa* strategically employs quorum sensing as an intracellular communication mechanism, orchestrating population density, gene expression, and biofilm formation. This intricate process hinges on the interplay of extracellular autoinducers, encompassing creation, detection, and response **(Smith & Iglewski, 2003).**

In the last decade, there has been a growing emphasis on creating novel therapeutics targeting *P. aeruginosa* infections. Notably, exploring natural compounds derived from traditional herbal sources has gained prominence as an efficacious strategy to counter the bacteria's distinctive resistance mechanisms. This pursuit involves a crucial hunt for new drugs and inhibitors, accentuating the significance of screening methodologies. Among these, virtual screening emerges as a pivotal facet of drug design, facilitating the identification and selection of promising compounds. By streamlining the process, virtual screening conserves time, resources, and expenses and bestows adaptability and predictability to the drug development trajectory. Traditional medical knowledge, which employs *S. lychnophora* fruits to treat pharyngitis and dry cough, implies the antibacterial potential of *S. lychnophora*. The study on the antibiofilm properties of *S. lychnophora* presented compelling evidence supporting its potential as a natural remedy against *Streptococcus* mutans, a pivotal contributor to dental caries and plaque formation (**Y. Yang *et al.*, 2016**). Extracts from both the husk and kernel of *S. lychnophora* demonstrated significant antibacterial activity in a dose-dependent manner, suggesting a promising avenue for combating the formation of dental plaque. Despite the progress made in understanding the antibiofilm properties of *S. lychnophora*, there needs to be more knowledge concerning the biologically active compounds within its extract and the molecular mechanisms by which these compounds impact bacterial biofilm formation. While the study, as mentioned earlier, demonstrated promising results against Streptococcus mutans, it is imperative to delve deeper into the molecular intricacies and ascertain the broad-spectrum antibacterial potential, particularly against common *P.aeruginosa* strains. This study seeks to investigate the active compounds of *S. lychnophora* and aims to elucidate their precise mechanisms of action on bacterial biofilm formation, particularly concerning *P. aeruginosa* strains, thereby significantly advancing our understanding.

MATERIAL AND METHODS

Materials

The dried fruits of *S. lychnophora*, known as 'hạt ươi' in Vietnamese, were procured from the Hiep Duc market in Quang Nam, Vietnam, in August 2018. This market is located in an area abundant with *S. lychnophora* forests, ensuring the authenticity of the botanical material. Dr. Nguyen Duc Huy carried out the authentication process at the Institute of Biotechnology, Hue University. A voucher specimen (SH2019-2) has been securely housed at the Biotechnology Laboratory, Da Nang University of Science and Technology, preserving the integrity of the research and providing a reliable resource for future studies.

The microorganisms used in this study were *P. aeruginosa* PAO1strains. Strains were maintained in Mueller-Hinton (MH) agar (Difco) at 4^0C until required for the study.

In silico screening of bioactivity of identified compounds from *S. lychnophora* Hance

A compilation of 55 compounds derived from *S. lychnophora* Hance was assembled by referencing previous works (Tab S1) **(Oppong *et al*., 2020; Oppong, Li, *et al*., 2018; R.-F. Wang *et al*., 2003; Zhao *et al*., 2008)**. The 3D structures of these compounds were acquired in sdf format from the PubChem database (https://pubchem.ncbi.nlm.nih.gov/). The Protein Databank was explored to find key structures of virulence factors of *P. aeruginosa (https://www.rcsb.org/)*. A total of 6 X-ray structures were selected as in Tab 1. Molecular docking studies were conducted using AutoDock Vina **(Trott & Olson, 2010)**, eliminating water molecules from protein crystal structures, adding hydrogen atoms, and calculating charges. The docking score was harnessed to assess the theoretical binding affinities between the chosen compounds and the designated vital targets. In all simulations, the docking grid spanned the entirety of the target protein's structure, facilitating unbiased predictions of binding sites for the identified "hit" compounds. Based on the AutoDock Vina scoring function, the top five compounds were subsequently selected for analysis using the molecular graphics program Pymol (**Schrödinger, LLC, 2015**) and specific interactions analysis by PLIP **(Adasme *et al*., 2021).** The ligand-protein interaction diagrams are presented by Ligplot **(Laskowski & Swindells, 2011).**

Table 1 Target protein for screening antibacterial activity of *S. lychnophora* Hance extracted compounds

Categories	*Virulence factors*	*Structure code*	*Functions*
Secreted factors	Alginate and lipopolysaccharide	1K2Y	Crystal Structure of Phosphomannomutase/Phosphoglucomutase S108A mutant from *P. aeruginosa*
	Elastase B	3DBK	*P. aeruginosa* elastase with phosphoramidon
Cell-cell interaction	Quorum sensing	4JVC	The PqsR ligand binding domain is in the apo form and in complex with its native agonist 2-nonyl-4-hydroxyquinoline.
		AF-Q9I4X3-F1	Crystal structure of the N-terminal domain of anthranilate-CoA ligase
		3QP1	Crystal structure of CviR ligand-binding domain bound to the native ligand C6-HSL
	Biofilm	2UV0	Structure of the P.*aeruginosa* LasR ligand-binding domain bound to its autoinducer

Preparation of *S. lychnophora* Hance dried fruits ethanol extract (SLHe)

Dried pericarp from *S. lychnophora* fruits (5g) were soaked with 500 mL of ethanol, 80% for 12h at room temperature, and then heated to 80^0C for 1h. The extracts obtained were filtered through a cloth filter to collect liquid extract. Afterward, they were concentrated to dryness under reduced pressure using a rotary evaporator at 50^0C. When used, it was diluted with DMSO 10%.

Biofilm production and inhibition assay

The biofilm production was determined using the method described by Christina Ebert **(Ebert *et al*., 2021)** with some modifications. The strains were activated through cultivation in 5 mL of Tryptic Soy Broth (TSB) at 37ºC for 24 hours. The optical density (OD) was gauged at 600 nm, and suitable dilutions were prepared in TSB supplemented with 1% sucrose to achieve an optical density of 0.1, corresponding to approximately 10^6 cells/mL. A volume of 100 µl of the *P. aeruginosa* cultures was dispensed into separate wells of flat-bottomed 96-well microtiter plates, which were then incubated at 37ºC without agitation. After 4 hours of incubation, 100 µl aliquots of SLHe diluted in TSB were introduced into the wells of the 96-well microtiter plates. Ampicillin functioned as the positive control, while DMSO served as the vehicle. After the 24-hour incubation, non-adherent cells were eliminated by gently immersing each sample three times in sterile phosphate-buffered saline (PBS). The samples were then fixed at 60ºC for 1 hour, followed by the staining of biofilms using a 0.1% crystal violet solution in water. Following staining, the samples underwent triple washing with distilled water. For the quantitative assessment of biofilm production, a solution of 30% acetic acid (125 µL) was added to destain the samples.

Afterward, the OD at 492 nm was detected. The percentage of biofilm inhibition was determined by the formula:

$$\text{Biofilm reduction \%} = (OD_{control} - OD_{sample})/(OD_{control}) \times 100\%$$

Pyocyanin assay

The pyocyanin assay was performed according to the method described by Essar *et al.* **(Ebert *et al*., 2021)**. *P. aeruginosa* was subjected to incubation both in the presence and absence of sub-MIC (Minimum Inhibitory Concentration) levels of SLHe at 37^0C for 48 hours. Subsequently, the culture media underwent centrifugation at 10,000 rpm for 15 minutes. 5 mL aliquot of the culture supernatant was subjected to extraction using 3 mL of chloroform, followed by re-extraction into 1 mL of 0.2N hydrochloric acid (HCl), yielding a solution displaying hues ranging from orange-yellow to pink. The absorbance of this solution was quantified at a wavelength of 520 nm.

Protease activity

P. aeruginosa was grown in nutrient broth supplemented with SLHe (0.125 – 0.4 mg/ml) or without extract. Following incubation, a volume of 400 µl of the supernatant was combined with an equivalent volume of 2% azocasein solution at pH 7. This mixture was then subjected to incubation at 37^0C for 1 hour. The reaction was halted by adding 500 µl of 10% trichloroacetic acid, and the reaction mixture was centrifuged at 8,000 g for 5 minutes to eliminate residual azocasein. Subsequently, the absorbance of the supernatant was measured at a wavelength of 400 nm.

The integrity of the cell membrane

The cellular material release was performed according to the method described by Yang *et al*. **(Yang *et al*., 2015**). SLHe at the MIC concentration were added to 2 mL of *P. aeruginosa* in sterilized peptone water (0.1 g/100 mL) and then incubated at 37^0C. At intervals of 0, 1, 2, 3, 4, 5, and 6 hours following treatment, the cells were harvested and subsequently subjected to centrifugation at 3000 rpm. The UV absorbance of the supernatant was quantified at 260 nm utilizing a spectrophotometer. A tube containing sterilized peptone water devoid of bacteria was employed as a control.

RESULTS AND DISCUSSION

In silico screening virulent factor targeted identified compounds from *S. lychnophora* -

Molecular docking studies were conducted to explore the binding affinities of 55 compounds of *S. lychnophora* with essential virulent factor proteins, including PMM/PGM, elastase B, PqsR, PqsA, CviR', and LasR. The highest binding affinity docking score (in kcal/mol) for each target protein is shown in Tab 2, and all docking scores are shown in Tab S1. The top 5 compounds that exhibit the highest binding affinities with the target proteins and the specific interactions analysis by PLIP **(Adasme *et al*., 2021)** are shown in Tab 3 and Tab 4. The protein-ligand interactions between the top compounds and the PqsA protein using Ligplot **(Laskowski & Swindells, 2011)** are represented in Fig.1.

Table 2 Highest binding affinity of the target protein with extracted compounds by docking

Target	*PqsA*	*PMM/PGM*	*CviR'*	*PqsR*	*LasR*	*Elastase B*
Protein structure ID	AF-Q9I4X3-F1	1K2Y	3QP1	4JVC	2UV0	3DBK
Highest binding affinity docking score (Kcal/mol)	-10.5	-9.2	-7.4	-6.1	-5.6	-5.2

Table 3 The top 5 compounds with the highest binding affinity to PqsA by docking

Compounds	*Synonyms name*	*Binding Affinity (Kcal/mol)*
Cosmosiin	Apigetrin, Apigenin 7-glucoside, Cosmetin	-10.5
Tiliroside	Tribuloside, Kaempferol-3-(p-coumaryl)glucoside	-10.5
Rhamnetin 3-laminaribioside	Quercetin 7-methyl ether 3-laminaribioside	-10.5
Kaempferol-3-O-rutinoside	Nictoflorin	-10.4
Cynaroside	Luteolin 7-glucoside, Luteoloside	-10.1

Table 4 The protein-ligand interaction analysis by PLIP

Compounds	*Hydrophobic Interactions*	*Hydrogen Bonds*	*π-Stacking*	*Salt Bridges*
Cosmosiin	4 (205, 209, 211, 254)	3 (211, 304, 378, 397)	1 (209)	1 (493)
Tiliroside	3 (211, 301, 493)	5 (279, 302, 304, 382, 397)	1 (493)	2(397, 493)
Rhamnetin 3-laminaribioside	4 (254, 493, 493, 494)	7 (256,280,415,428,488,494, 496)		1 (488)
Kaempferol-3-O-rutinoside		9 (172, 210,211, 304, 305, 372, 378,397, 493)		2 (397, 493)
Cynaroside	4 (205, 209, 211, 254)	5 (211, 302, 304, 380, 397)	1 (209)	1 (493)

The docking simulation between the protein and ligand yielded a favorable binding affinity of -10.5 kcal/mol, indicating a strong interaction. The binding interface revealed interactions observed, including hydrophobic interactions, hydrogen bonds, and π-stacking. These findings suggest a robust and diverse set of interactions between the protein and ligand, highlighting their potential for forming stable complexes. The hydrophobic interactions contribute to the nonpolar contacts between the molecules, while the hydrogen bonds enhance the specificity and strength of the binding. Additionally, the π-stacking interaction and salt bridge further stabilize the complex formation. These results provide valuable insights into the molecular interactions underlying the protein-ligand binding, suggesting a promising basis for further exploration and development of potential therapeutic agents.

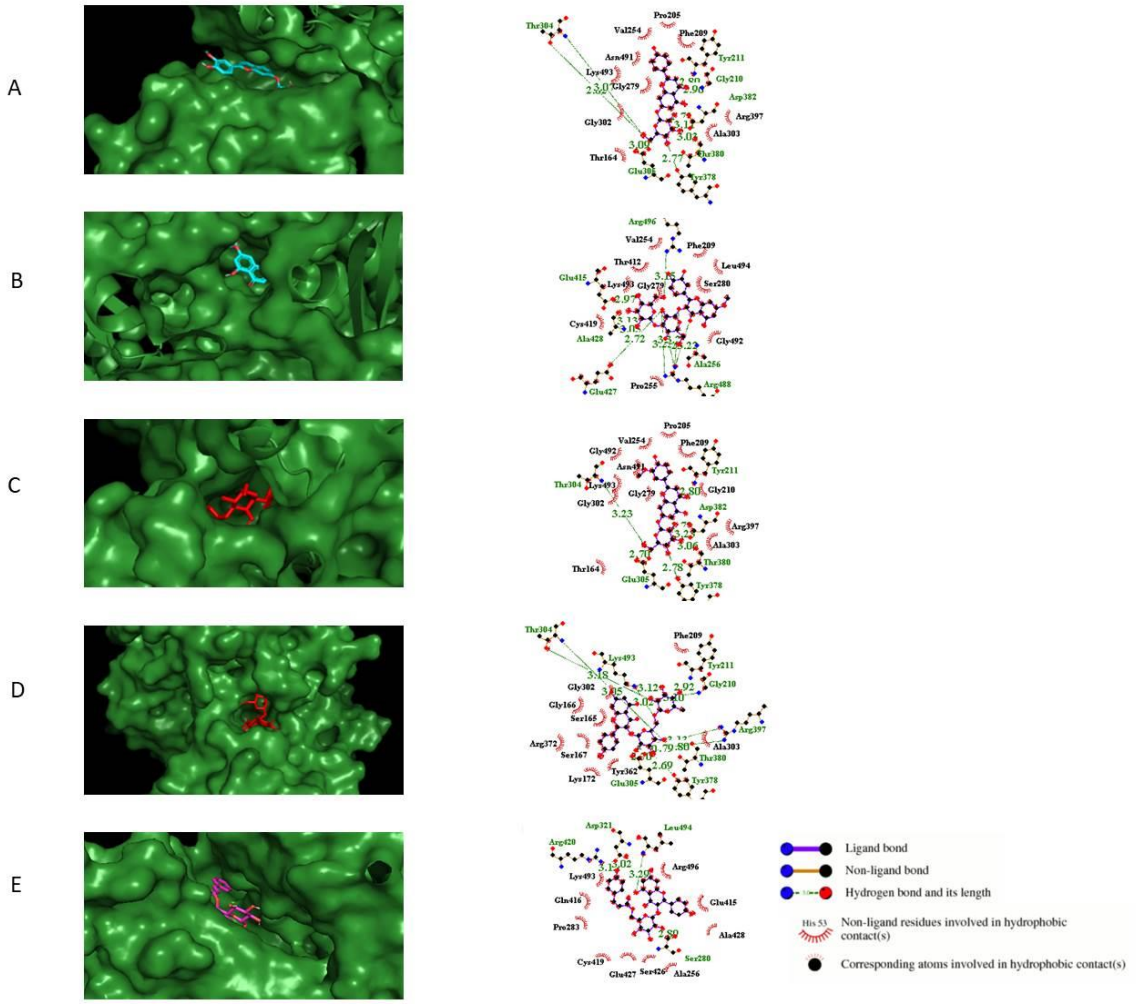

Figure 1 Visualizing the interaction between PqsA (AF-Q9I4X3-F1) and the top 5 ligands with the highest binding affinity.
Left: PyMOL representation depicting the location of the selected compound on the surface of PqsA.
Right: Ligplot analysis results showing the 2D representation of protein-ligand interactions for PqsA and 5 selected compounds. A-Cosmosiin; B- Tiliroside;C-Rhamnetin 3-laminaribiosid; D-Kaempferol-3-O-rutinoside; E-Cynaroside

The docking analysis identified several compounds with bioactive potential, including Cosmosiin, Tiliroside, Rhamnetin 3-laminaribioside, Kaempferol-3-O-rutinoside, and Cynaroside. Cosmosiin (Apigenin 7-O-beta-D-glucoside) is a glycosyloxyflavone in which apigenin is linked to a beta-D-glucopyranosyl moiety at position 7 via a glycosidic linkage. This compound exhibits the properties of a non-steroidal anti-inflammatory drug and an antibacterial agent **(Nabi *et al.*, 2019)**. Tiliroside, a flavonoid in various edible plants or specific plant components, has been the subject of prior investigations showcasing its anti-inflammatory properties **(Corrêa *et al.*, 2018)**. Rhamnetin (2-(3,4-dihydroxyphenyl)-3,5-dihydroxy-7-methoxychromen-4-one), classified as a secondary metabolite belonging to the flavonoid class, is present in a range of plants and fruits. Notably, it exhibits diverse pharmacological attributes, encompassing antioxidant, anticancer, anti-inflammatory, antiviral, and antibacterial activities **(Lee *et al.*, 2022)**. Kaempferol-3-O-rutinoside stands out as a potent in vitro inhibitor of α-glucosidase, displaying more than eight-fold greater activity than acarbose **(Habtemariam, 2011)**. Cynaroside is a flavonoid glycoside compound that is abundantly distributed in various plants and acknowledged for its multifaceted pharmacological effects. It assumes a pivotal role across different systems, including the respiratory, cardiovascular, and central nervous systems **(Ji *et al.*, 2021)**.

The pqsA gene in *P. aeruginosa* plays a crucial role in producing the Pqs, a 3-hydroxy-4-quinolone involved in intercellular signaling and regulation of virulence genes (**J. Lin *et al.*, 2018)**. The PqsA protein serves as an anthranilate-CoA ligase, facilitating the priming of anthranilate for its incorporation into the Pqs biosynthetic pathway. Disruption of the PqsA enzyme's functionality can impede the synthesis of the Pqs signal molecule, consequently restraining PqsR-dependent gene regulation and ultimately thwarting biofilm formation **(Coleman *et al.*, 2008)**. The Pqs system operates as a vital conduit connecting the Las and Rhl quorum sensing systems, exerting a comprehensive regulatory influence on *P. aeruginosa*. Its impact extends to various physiological processes and virulence factors. Inhibiting PqsA activity disrupts the generation of the Pqs signal molecule, leading to the curtailment of virulence factors and the subsequent inhibition of biofilm formation.

Validation of biofilm formation inhibition and biofilm destruction activity of SLHe

The docking results provided insight into the binding affinities between the compounds from SLHe and the target protein PQSA, suggesting their potential inhibitory effects on biofilm formation. SLHe exhibited the antimicrobial activity of *P. aeruginosa*, and the MIC value of SLHe on *P. aeruginosa* was identified at 4mg/ml. We further examined the anti-biofilm of SLHe in the concentration under MIC value. The results from the wet experiment demonstrated that SLHe effectively inhibits biofilm formation in *P. aeruginosa* (Tab 5).

Table 5 Antibiofilm formation and destruction activity of SLHe against *P. aeruginosa*

SLHE (mg/ml)	*Antibiofilm formation (%)*	*Biofilm destruction (%)*
4	55.86 ± 3.16^{a}	42.8 ± 2.46^{a}
2	42.53 ± 4.21^{b}	35.23 ± 2.54^{b}
1	27.46 ± 0.96^{c}	22.78 ± 2.05^{c}
0.5	13.40 ± 0.96^{d}	9.45 ± 1.96^{d}
0.25	6.36 ± 2.53^{e}	5.36 ± 2.78^{e}
0.125	3.83 ± 1.71^{e}	2.98 ± 2.81^{e}
Ampicilin 0.25	1.06 ± 1.23^{e}	2.09 ± 2.04^{e}

Each value represents mean ± SE. Antibiofilm formation and biofilm destruction mean ± SD followed by different letters with in a column indicate significance differences according to ANOVA and Turkey HSD test ($p<0.05$)

At a concentration of 4 mg/ml, SLHe reduced biofilm formation by 55.86%. The control, ampicillin, showed a biofilm reduction of only 1,06%. Moreover, the biofilm destruction activity of SLHe was also investigated, and the results were equally encouraging. At a concentration of 4 mg/ml, SLHe decreased biofilm formation by 42.8%. The combined findings demonstrate the dual effectiveness of SLHe against *P. aeruginosa* biofilms. It exhibits significant antibiofilm formation activity, preventing biofilm development, and also demonstrates potent biofilm destruction activity, breaking down existing biofilms. These results underscore the potential of SLHe as a promising alternative to traditional treatments and highlight the need for further research to fully understand its mechanisms and explore its clinical applications.

Evaluation of the effect of SLHe on pyocyanin and protease secretion in *P. aeruginosa*

Next, we assessed the impact of SLHe on the secretion of bacterial virulence factors, specifically proteases and pyocyanin. SLHe displayed anti-quorum sensing activity against the reference strain *P. aeruginosa*. Various concentrations were utilized to measure the inhibition of pyocyanin, a quorum sensing activity indicator (Fig 2).

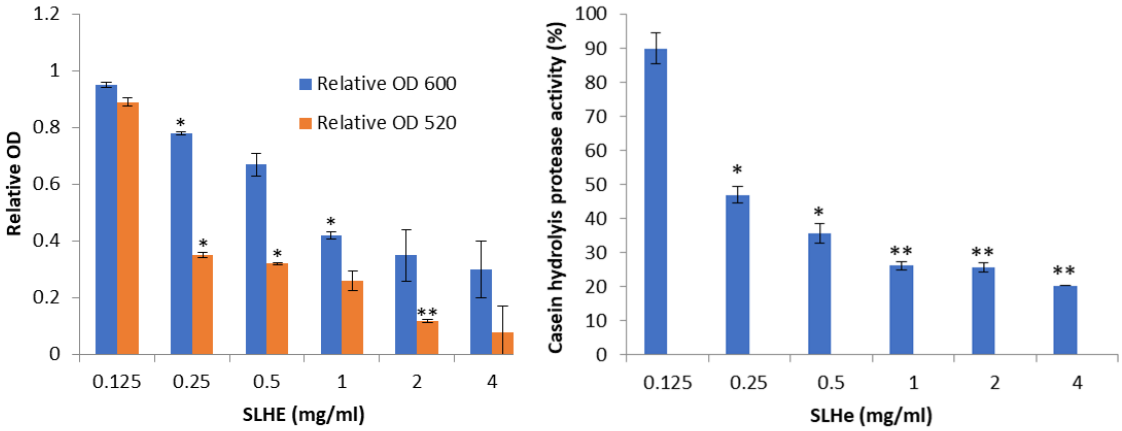

Figure 2 Effect of different concentrations of SLHe on Pyocyanin production and protease activity.
Left: Optical density and Pyocynn of *P. aeruginosa* culture exposed to different concentrations of SLHe, respectively. Error bars indicate SEM. Statistically significant differences ($p < 0.05$, Tukey test) from the control sample are indicated with *.
Right: Degree of hydrolysis of casein hydrolyzed under different SLHe concentrations (at 0.125, 0.25, 0.5, 1, 2, 4 mg/ml). Error bars are expressed as mean ± standard error with $n \geq 3$. In each graph, the * represents significant differences ($p < 0.05$) in the degree of hydrolysis values.

The production of pyocyanin decreased progressively with increasing concentrations of the extract, reaching approximately 95% inhibition at 0.4 mg/mL. Moreover, the casein hydrolytic protease assay revealed a notable reduction in protease activity in SLHe-treated cells compared to untreated cells. Quantitatively, it was observed that a concentration of 4 mg/mL SLHe resulted in the minimum release of protease by *P. aeruginosa*.

Effect of SLHe on pH modulation and cell material release in *P. aeruginosa*

Release cell material from *P. aeruginosa* treated with SLHe is depicted in Fig 3. SLHe treatment caused an increasing release of cell materials according to exposure time. It has been reported that *P. aeruginosa* produces some organic acids, such as alginic acid and l-guluronic acid. *P. aeruginosa* generally forms more biofilm and induces antibiotic resistance faster in acidic conditions**(Q. Lin *et al.*, 2021)**. SLHe inhibited the decrease in pH induced by *P. aeruginosa*, suggesting that the SLHe may inhibit the organic acid production of P. aeruginosa, thus decreasing biofilm formation.

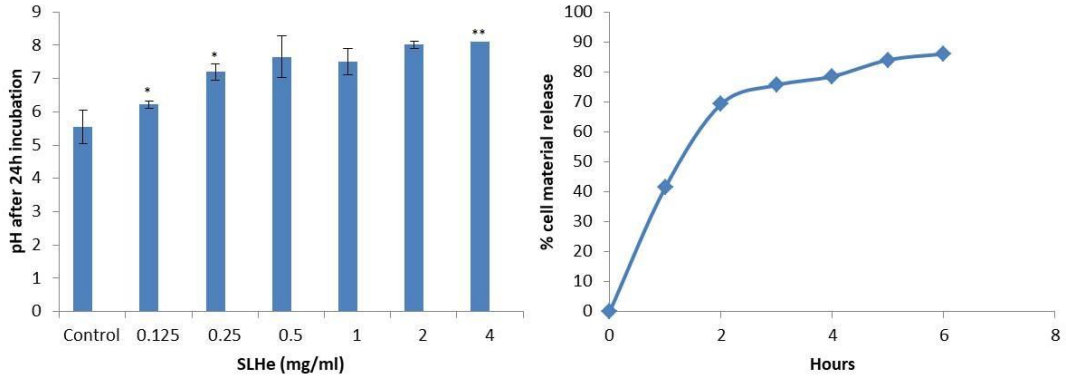

Figure 3 Effect of SLHe on pH modulation and cell material release in *P. aeruginosa*
Different concentration of SLHe (0.125−0.4 mg/ml) was used to quantify the pH and cell material release of *P. aeruginosa*. Cultures without the extract were considered as a control. *Indicates significant differences from the control at P < 0.05.

This study sheds light on the bioactive potential of *S. lychnophora* Hance, particularly its ethanol extract. Little attention has been given to the ethanol extract of *S. lychnophora* Hance, leading to a significant knowledge gap in scientific understanding, as previous studies have primarily focused on the polysaccharides present in this plant. Through docking analysis, it was found to have a high binding affinity with quorum signaling proteins, suggesting its potential to disrupt bacterial communication and coordination of virulence factors. SLHe exhibited inhibiting the growth of bacteria. It also showed the ability to disrupt biofilm formation, vital for establishing chronic infections. The extract exhibited a dual effect by decreasing the virulence of P.*aeruginosa*, reducing pyocyanin production, and inhibiting protease activity, indicating its potential to interfere with key virulence factors. The present study highlights the importance of conducting further phytochemical investigations on the organic extracts of *S. lychnophora* Hance to elucidate the secondary metabolites present. Additionally, it is crucial to conduct bioactivity studies on these metabolites to determine their specific roles in the observed effects attributed to *S. lychnophora* Hance. By bridging this knowledge gap and gaining a better understanding of the bioactive components, we can unlock the full therapeutic potential of *S. lychnophora* Hance and explore its potential applications in medicine and healthcare.

CONCLUSION

The present research underscores the high feasibility of employing bioinformatics tools to predict the activity and mechanism of natural compounds accurately. The synergy between computational predictions and in vitro experimental validations further solidifies the results' reliability. This integrated approach not only enhances our understanding of compound functionality but also paves the way for more efficient and informed exploration of potential applications in various domains. The study demonstrated that the SLHe on biofilm formation and virulence factors secretory of *P. aeruginosa*, potentially through its binding to anthranilate-CoA ligase and subsequent regulated pyocyanin production. The results provided a comprehensive understanding of the antimicrobial mechanism of SLHe, especially on biofilm pathogens. These findings contributed valuable insights for further exploring and developing potential therapeutic agents and strategies targeting bacterial infections and their associated virulence factors.

Acknowledgments: We thank Dr. Nguyen Thi Dong Phuong, Food Chemistry Faculty, Da nang University of Science and Technology for kindly providing the PAO1 strains. We are grateful to the Reviewers for their constructive criticisms of the manuscript**.** This study is supported by 2022-2023 DUT-NCKU Joint Research Program under grant number 01/HTQT/2023.

REFERENCES

Adasme, M. F., Linnemann, K. L., Bolz, S. N., Kaiser, F., Salentin, S., Haupt, V. J., & Schroeder, M. (2021). PLIP 2021: expanding the scope of the protein–ligand interaction profiler to DNA and RNA. *Nucleic Acids Research*, *49*(W1), W530–W534. https://doi.org/10.1093/nar/gkab294

Coleman, J. P., Hudson, L. L., McKnight, S. L., Farrow, J. M. 3rd, Calfee, M. W., Lindsey, C. A., & Pesci, E. C. (2008). Pseudomonas aeruginosa PqsA is an anthranilate-coenzyme A ligase. *Journal of Bacteriology*, *190*(4), 1247–1255. https://doi.org/10.1128/JB.01140-07

Corrêa, W. R., Serain, A. F., Aranha Netto, L., Marinho, J. V. N., Arena, A. C., Figueiredo de Santana Aquino, D., Kuraoka-Oliveira, Â. M., Júnior, A. J., Bernal, L. P. T., Kassuya, C. A. L., & Salvador, M. J. (2018). Anti-Inflammatory and Antioxidant Properties of the Extract, Tiliroside, and Patuletin 3-O-β-D-Glucopyranoside from Pfaffia townsendii (Amaranthaceae). *Evidence-Based Complementary and Alternative Medicine : ECAM*, *2018*, 6057579. https://doi.org/10.1155/2018/6057579

Díaz-Pérez, S. P., Solis, C. S., López-Bucio, J. S., Valdez Alarcón, J. J., Villegas, J., Reyes-De la Cruz, H., & Campos-Garcia, J. (2023). Pathogenesis in Pseudomonas aeruginosa PAO1 Biofilm-Associated Is Dependent on the Pyoverdine and Pyocyanin Siderophores by Quorum Sensing Modulation. *Microbial Ecology*, *86*(1), 727–741. https://doi.org/10.1007/s00248-022-02095-5

Ebert, C., Tuchscherr, L., Unger, N., Pöllath, C., Gladigau, F., Popp, J., Löffler, B., & Neugebauer, U. (2021). Correlation of crystal violet biofilm test results of Staphylococcus aureus clinical isolates with Raman spectroscopic read-out. *Journal of Raman Spectroscopy*, *52*(12), 2660–2670. https://doi.org/https://doi.org/10.1002/jrs.6237

Habtemariam, S. (2011). A-glucosidase inhibitory activity of kaempferol-3-O-rutinoside. *Natural Product Communications*, *6*(2), 201–203.

Ji, J., Wang, Z., Sun, W., Li, Z., Cai, H., Zhao, E., & Cui, H. (2021). Effects of Cynaroside on Cell Proliferation, Apoptosis, Migration and Invasion through the MET/AKT/mTOR Axis in Gastric Cancer. *International Journal of Molecular Sciences*, *22*(22). https://doi.org/10.3390/ijms222212125

Kawk, H. W., Nam, G.-H., Kim, M. J., Kim, S.-Y., & Kim, Y.-M. (2021). Scaphium affine Ethanol Extract Induces Anoikis by Regulating the EGFR/Akt Pathway in HCT116 Colorectal Cancer Cells. *Frontiers in Oncology*, *11*, 621346. https://doi.org/10.3389/fonc.2021.621346

Laskowski, R. A., & Swindells, M. B. (2011). LigPlot+: multiple ligand-protein interaction diagrams for drug discovery. *Journal of Chemical Information and Modeling*, *51*(10), 2778–2786. https://doi.org/10.1021/ci200227u

Lee, H., Krishnan, M., Kim, M., Yoon, Y. K., & Kim, Y. (2022). Rhamnetin, a Natural Flavonoid, Ameliorates Organ Damage in a Mouse Model of Carbapenem-Resistant Acinetobacter baumannii-Induced Sepsis. In *International Journal of Molecular Sciences* (Vol. 23, Issue 21). https://doi.org/10.3390/ijms232112895

Li, C. (2015). *Sterculia lychnophora Hance 胖大海 (Pangdahai, Malva Nut Tree) BT - Dietary Chinese Herbs: Chemistry, Pharmacology and Clinical Evidence* (Y. Liu, Z. Wang, & J. Zhang (eds.); pp. 535–542). Springer Vienna. https://doi.org/10.1007/978-3-211-99448-1_61

Liao, C., Huang, X., Wang, Q., Yao, D., & Lu, W. (2022). Virulence Factors of Pseudomonas Aeruginosa and Antivirulence Strategies to Combat Its Drug Resistance In *Frontiers in Cellular and Infection Microbiology* (Vol. 12). https://www.frontiersin.org/articles/10.3389/fcimb.2022.926758

Lin, J., Cheng, J., Wang, Y., & Shen, X. (2018). The Pseudomonas Quinolone Signal (PQS): Not Just for Quorum Sensing Anymore. *Frontiers in Cellular and Infection Microbiology*, *8*. https://doi.org/10.3389/fcimb.2018.00230

Lin, Q., Pilewski, J. M., & Di, Y. P. (2021). Acidic Microenvironment Determines Antibiotic Susceptibility and Biofilm Formation of Pseudomonas aeruginosa. *Frontiers in Microbiology*, *12*, 747834. https://doi.org/10.3389/fmicb.2021.747834

Nabi, B., Rehman, S., Baboota, S., & Ali, J. (2019). 9 - Natural antileprotic agents: a boon for the management of leprosy. In G. B. T.-D. and D. of T. from N. P. A. N. T. D. Brahmachari (Ed.), *Natural Product Drug Discovery* (pp. 351–372). Elsevier. https://doi.org/https://doi.org/10.1016/B978-0-12-815723-7.00009-2

Ogale, S. C., Kasture, S. B., Kasture, V. S., & Tiwari, R. (2014). Screening of methanol extract of Sterculia scaphigera wall seeds for ulcerprotective and antioxidation acivity. *4*(01), 1332–1346.

Oppong, M. B., Li, Y., Banahene, P. O., Fang, S.-M., & Qiu, F. (2018). Ethnopharmacology, phytochemistry, and pharmacology of Sterculia lychnophora Hance (Pangdahai). *Chinese Journal of Natural Medicines*, *16*(10), 721–731. https://doi.org/10.1016/S1875-5364(18)30112-2

Oppong, M. B., LI, Y., Banahene, P. O., FANG, S. M., & QIU, F. (2018). Ethnopharmacology, phytochemistry, and pharmacology of Sterculia lychnophora Hance (Pangdahai). *Chinese Journal of Natural Medicines*. https://doi.org/10.1016/S1875-5364(18)30112-2

Oppong, M. B., Zhang, B.-Y., Fang, S.-M., & Qiu, F. (2020). Secondary metabolites from Sterculia lychnophora Hance (Pangdahai). *Biochemical Systematics and Ecology*, *92*, 104125. https://doi.org/https://doi.org/10.1016/j.bse.2020.104125

Palve, A., Shetty, P., Pimpliskar, M., & Jadhav, R. N. (2016). *Study on Antibacterial and Antifungal Activities of Sterculia lychnophora Extracts Original Research Article Study on Antibacterial and Antifungal Activities of Sterculia lychnophora Extracts*. *January*.

Panomai, N. (2018). Malva nut (Scaphium scaphigerum) beverage consumption on food intake and waist circumference. *Journal of Applied Sciences Research*, *14*(May 2012), 13–17. https://doi.org/10.22587/jasr.2018.14.3.3

Pimpliskar, D. R. M. (2014). IN-SIlico Docking Analysis of Sterculia Lychnophora Compounds against Proteins Causing Alzheimer's Disease. *International Journal of Engineering Science and Innovative Technology (IJESIT)*, *3*, 158–164.

Qin, S., Xiao, W., Zhou, C., Pu, Q., Deng, X., Lan, L., Liang, H., Song, X., & Wu, M. (2022). Pseudomonas aeruginosa: pathogenesis, virulence factors, antibiotic resistance, interaction with host, technology advances and emerging therapeutics. *Signal Transduction and Targeted Therapy*, *7*(1), 199. https://doi.org/10.1038/s41392-022-01056-1

Schrödinger, LLC. (2015). *The {AxPyMOL} Molecular Graphics Plugin for {Microsoft PowerPoint}, Version~1.8*.

Smith, R. S., & Iglewski, B. H. (2003). Pseudomonas aeruginosa quorum sensing as a potential antimicrobial target. *The Journal of Clinical Investigation*, *112*(10), 1460–1465. https://doi.org/10.1172/JCI20364

Trott, O., & Olson, A. J. (2010). AutoDock Vina: improving the speed and accuracy of docking with a new scoring function, efficient optimization, and multithreading. *Journal of Computational Chemistry*, *31*(2), 455–461. https://doi.org/10.1002/jcc.21334

Vestby, L. K., Grønseth, T., Simm, R., & Nesse, L. L. (2020). Bacterial Biofilm and its Role in the Pathogenesis of Disease. *Antibiotics (Basel, Switzerland)*, *9*(2). https://doi.org/10.3390/antibiotics9020059

Wang, R.-F., Yang, X.-W., Ma, C.-M., Shang, M.-Y., Liang, J.-Y., Wang, X., Cai, S.-Q., & Shoyama, Y. (2003). Alkaloids from the Seeds of Sterculia lychnophora (Pangdahai). *ChemInform*. https://doi.org/10.1002/chin.200338184

Wang, R. F., Wu, X. W., & Geng, D. (2013). Two cerebrosides isolated from the seeds of Sterculia lychnophora and their neuroprotective effect. *Molecules*. https://doi.org/10.3390/molecules18011181

Wu, Y., Cui, S. W., Wu, J., Ai, L., Wang, Q., & Tang, J. (2012). Structure characteristics and rheological properties of acidic polysaccharide from boat-fruited sterculia seeds. *Carbohydrate Polymers*, *88*(3), 926–930. https://doi.org/https://doi.org/10.1016/j.carbpol.2012.01.035

Yang, X.-N., Khan, I., & Kang, S. C. (2015). Chemical composition, mechanism of antibacterial action and antioxidant activity of leaf essential oil of Forsythia koreana deciduous shrub. *Asian Pacific Journal of Tropical Medicine*, *8*(9), 694–700. https://doi.org/10.1016/j.apjtm.2015.07.031

Yang, Y., Park, B.-I., Hwang, E.-H., & You, Y.-O. (2016). Composition Analysis and Inhibitory Effect of *Sterculia lychnophora* against Biofilm Formation by *Streptococcus mutans*. *Evidence-Based Complementary and Alternative Medicine*, *2016*, 8163150. https://doi.org/10.1155/2016/8163150

Zhao, W.-H., Zhao, C.-Y., Gao, L.-F., Feng, F.-F., Gao, W., Chen, Z.-L., Zhang, F., Cao, L.-G., Bi, X.-Y., Chen, Y., Zhu, Q.-Y., & Zhang, Y.-X. (2008). The novel inhibitory effect of Pangdahai on fatty acid synthase. *IUBMB Life*, *60*(3), 185–194. https://doi.org/10.1002/iub.28

Supplementaty data:

Table S1 *55 compounds derived from S. lychnophora Hance and docking scores with 6 targets protein in biofilm signaling of P.aeruginosa*

	Binding affinity (Kcal/mol)					
Derived compounds from S. lychnophora Hance	*PQSA* AF-Q9I4X3-F1	*PMM/PGM* 1K2Y	*CviR'* 3QP1	*PqsR* 4JVC	LasR 2UV0	Elastase 3DBK
n-Eicosanoic acid	-5.9	-4.6	-4.5	-4.5	-3.8	-5.1
Succinic Acid	-4.9	-4.7	-4.7	-4.8	-5.4	-5.1
Tetracosanoic acid	-5.9	-4.4	-4.3	-5	-4.4	-4.6
Apigenin 7-glucoside	-10.5	-7.4	-6.3	-6	-5.8	-4.6
Pentadecanoic acid	-5.4	-4.6	-4.6	-4.2	-3.7	-4.4
2-methylheptanoic acid	-4.8	-4.4	-4.6	-4.3	-4.4	-5.2
2,4 dihydroxybenzoic acid	-6.2	-5.8	-5.4	-6	-5.6	-4.7
4-Methylhexanoic acid	-4.7	-4.8	-4.3	-4.4	-5.5	-4.9
15-methylhexadecanoic acid	-6.1	-4.8	-4.3	-4.5	-4.3	-4.9
Tricosanoic acid	-5.9	-4.3	-4.2	-5.1	-4	-4.4
2-Methylhexanoic acid	-4.7	-5	-5.6	-4.4	-4.6	-4.7
β-sitosterol	-10	-7.2	-6.3	-6.8	-5.6	-4.6
nonanedioic acid	-5.2	-6	-4.4	-4.7	-4.6	-4.3
kaempferol-3-O-β-D-glucoside	-8.8	-8.1	-6.5	-6.1	-6.7	-4.3
L-Rhamnose	-5.8	-5.5	-5.7	-5.7	-5	-5.1
Decanoic acid	-5	-5.8	-4.1	-4.3	-5.5	-5.1
(Z)-11-hexadecanoic	-5.6	-4.2	-4.1	-3.9	-3.6	-3.8
8-Nonynoic acid	-5	-4.1	-4.2	-4.2	-4.6	-4.6
Octanoic acid	-4.7	-4.9	-4.1	-4.2	-4.6	-4.9
2-(hydroxymethyl)-5-hydroxypyridine	-5.5	-5.1	-5.1	-5.2	-5.3	-4.4
(Z)-9-Octadecenoic acid	-6	-4.6	-4.2	-4.7	-4.1	-4.7
Vomifoliol	-6.6	-6.7	-4.9	-5	-5.2	-4.5
Luteolin 7-glucoside	-10.1	-8.3	-7.4	-5.3	-5.5	-5.2
(Z)-7-Octadecenoic acid	-9.8	-8	-7.2	-5.4	-5.2	-5.1
Octadecanoic acid	-6.2	-4.8	-4.2	-4.7	-3.7	-4.4
(Z)-7-Octadecenoic acid	-6.3	-4.5	-5	-5	-4.4	-5.1
(Z)-5-Octadecenoic acid	-6.2	-4.6	-4.6	-4.7	-5.4	-4.8
Cis-10-nonadecenoic acid	-6.2	-4.9	-4.9	-5.3	-4.3	-4.3
Isorhamnetin-3-O-β-D-rutinoside	-10.5	-8.1	-6.4	-6.1	-5.2	-5.1
Kaempferol-3-O-β- D-rutinoside	-10.4	-8.9	-7.2	-5.6	-5.6	-5.1
Tiliroside	-10.5	-9.2	-6.6	-5.9	-5.5	-5.1
(Z)-11-Eicosanoic acid	-5.9	-4.2	-4.5	-5.4	-3.9	-4.6
Sitogluside	-9.8	-7.7	-6.6	-5.7	-4.7	-4.9
Sucrose	-6.3	-7.4	-5.8	-5.5	-5.1	-4.3
Uridine	-7.4	-6.5	-5.6	-5.3	-5.4	-4.8
D-Galactose	-5.9	-5.8	-5.7	-5.8	-5.4	-5.2
β-adenosine	-7.4	-6.8	-6.1	-5.6	-5.2	-5.1
Sterculinine I	-6.1	-4.8	-4.2	-4.7	-4.2	-4.6
Sterculinine II	-6.7	-7.5	-5.2	-6.1	-5.1	-4.7
(Z)-9-Hexadecenoic acid	-5.9	-4.4	-4.2	-4.9	-3.6	-4.1
Soya- cerebroside I	-6.9	-5.4	-5	-5.6	-5	-5.2

Caffeic acid	-6.6	-6	-5.8	-5.9	-5.6	-5.2
2-Furoic acid	-4.9	-4.9	-4.7	-5	-4.6	-4.6
Protocatechuic acid	-6.3	-5.9	-5.8	-5.6	-5.4	-5.1
Pinoresinol	-8.2	-7.7	-6.2	-6.1	-5.2	-4.6
9-Oxononanoic acid	-4.9	-5.2	-4.3	-4.5	-5.3	-4.7
(Z,Z)-9,12-Octadecenoic acid	-5.3	-4.4	-4.4	-4.7	-3.2	-4.5
Ethyl 3,4-dihydroxybenzoate	-6.1	-5.7	-6	-5.6	-5.4	-4.4
Heptanoic acid	-4.7	-4.4	-4.1	-4.1	-5.4	-4.4
Nonanoic acid	-5	-5.4	-4.2	-4.2	-5.2	-4.5
Undecanoic acid	-5.4	-5	-4.1	-4.5	-4.1	-4.6
Ethyl 2,4-dihydroxybenzoate	-6.4	-5.9	-5.6	-5.2	-4.6	-4.7
Docosanoic acid	-5.8	-4.5	-4.7	-4.4	-3.9	-5.1
(Z)-11-hexadecanoic	-5.4	-6.2	-4.3	-4.9	-5.1	-4.9
3-methyl-heptanedioic acid	-5.1	-5	-5	-4.5	-4.6	-5.1